Kepes
http://scholopress.com/kepes-journal

2023 Volume 21 Issue 3 pp. 393-411

Cannabidiol as a Potential Anticancer Agent:
DFT, Molecular Docking and ADMET Proprieties Evaluation

Soumaya Aissaoui [1], **Halima Hajji** [2], ***Hanane Zaki** [1], **Marwa Alaqarbeh** [3], **Samir Chtita** [4], **Tahar Lakhlifi** [2], **Mohammed Aziz Ajana** [2], **Mohammed Bouachrine** [1,2]

[1]Biotechnology, Bioresources and Bioinformatics Laboratory, Higher School of Technology-Khenifra, University of Sultan My Slimane, PB 170, Khenifra 54000, Morocco

[2]Molecular Chemistry and Natural Substances Laboratory, department of chemistry, Faculty of Science, My Ismail University, Meknes, Morocco

[3]Laboratory of Chemistry-Biology Applied, National Agricultural Research Center, Al Baqa 19381, Jordan

[4]Laboratory of Analytical and Molecular Chemistry, Faculty of Sciences Ben M'Sik, Hassan II University of Casablanca, Casablanca 7955, Morocco

Abstract

In this work, molecular docking was performed to evaluate the anticancer activities of cannabidiol on various targeted proteins. Interactions and significant binding energy prove that cannabidiol can be synthesized and tested as a potent drug that treats all types of human cancer safely. The data obtained highlight the key amino acids involved in the ligand/protein interactions and show that the designed cannabidiol-bound complexes exhibited the best confirmation in the binding site. In addition, a DFT optimization of the geometry and orbital frontier analysis was performed to describe the chemical reactivity of the studied molecule. A pharmacokinetic and bioavailability study in the body was performed by ADMET proprieties. The results of the molecular docking indicate that cannabinol can tested as a potent drug to treat human cancer, given its interactions and significant binding energy up to -8,6 kcal/mol with FAAH protein.

Keywords: Cannabidiol, Anticancer, Molecular docking, DFT, ADMET

1. Introduction

The medicinal use of *Cannabis sativa* has a long history dating back to ancient times in China because it contains more than 100 different chemical compounds and represents a great academic and pharmaceutical interest (Brand & Zhao, 2017; Clarke & Merlin, 2015). *Cannabis sativa* is considered the main source of phytocannabinoids, and more than 100 different types of secondary metabolized active compounds are known as tetrahydrocannabinol (THC) and cannabidiol (CBD) (Andradas et al., 2021). THC is known for its psychoactive properties, while CBD is not psychoactive but has anti-tumor activity (Lichtor, 2015). Also, CBD has antioxidant and anti-inflammatory properties (Atalay et al., 2020).

CBD's pharmacological effects are due to its ability to mimic endogenous cannabinoids (endocannabinoids), which are mediated by specific cannabinoid receptors (Sharafi G et al., 2019). In addition, CBD acts on multiple targets other than CB1/CB2, where it can bind to other transmembrane proteins, including

*Corresponding author

DOI https://doi.org/10.5281/zenodo.7936583#100

the orphan G protein-coupled receptor 55 (GPR55), peroxisome proliferator-activated receptors (PPARs), and transient receptor potential vanilloid channels (TRPV1/TRPV2) (Almeida & Devi, 2020) . Also, CBD induces apoptosis by modulating numerous pro- and anti-apoptotic proteins and reducing tumor growth (Jeong, Yun, et al., 2019). In addition to its ability to inhibit several cancer factors, including 5-HT1A, Becl1, COX-2, DR5, EGF, FAAH, ICAM-1, NOS3, NOXA, PAI-1, RERK, and TIMP-1 (Seltzer et al., 2020, Kis et al., 2019).

The 5-HT1A receptor has been widely implicated in carcinogenesis and thus has been implicated in many types of human tumors, including prostate, bladder, small cell lung, colon, and cholangiocarcinoma (Corvino et al., 2018). 5-HT1A receptor antagonists have been shown to block the activities of 5HT, PI3K/AKT, and MAPK but mediate pathways of JAK/STAT antitumor immune responses through various receptors (Ye et al ., 2021). The Beclin-1 protein is essential for the induction of autophagy (Giatromanolaki et al ., 2018). CB1 and CB2 exert antitumor effect s by suppressing the NF-κB signaling pathway and increasing apoptotic cell death (Khunluck et al., 2022). Overexpression of COX-2 increases angiogenesis, migration, invasiveness, and tumor-induced immunosuppression and prevents apoptosis (Li et al., 2020), and DR5-target can induce apoptosis (Hou et al., 2022). Epidermal growth factor receptor (EGFR) activity promotes tumor growth, invasion, and metastasis. This justifies efforts to inhibit EGFR signaling (Muthusami et al., 2022). FAAH inhibitors in several cancer cell lines inhibit growth and proliferation, reduce migration, and have invasion properties (Brunetti et al., 2019). GPR55 is involved in oncogenic processes such as cell proliferation, differentiation, migration, invasion, and metastasis, which are altered in some cancer cells. Overexpression or high expression of GPR55 is correlated with cancer aggressiveness (Calvillo-Robledo et al., 2022). ICAM-1 can promote metastasis, stimulate proliferation, angiogenesis, and invasion, and combat apoptosis in cancer cells (Singh et al., 2021).

ICAM-1 expression downregulation can inhibit cell migration and invasion, and NOS3 is critical in autophagic cell death induced by CBD production (Jeong, Kim, et al., 2019). Noxa is important in regulating apoptosis in CBD-induced cells, induces cytotoxicity through inhibition of PAI-1 expression, decreases proliferation, migration, and invasive potential of lung cancer cells, and suppresses angiogenesis and metastasis formation (Jeong et al., 2019, Drozd et al., 2022).

PERK plays a vital role in the induction of apoptosis mediated by CBD (Fan & Jordan, 2022). It has been reported that PPARG can promote cancer progression by maintaining redox balance and promoting cell survival; blocking PPARG function leads to apoptosis (Liu et al., 2022). TIMP-1 activity is observed in various tumor tissues as an important indicator of invasion and metastasis (He et al., 2018). TRPV1 reduces cell growth and increases apoptosis, and TRPV2 expression increases cancer aggressiveness by promoting migration (Hou et al., 2019, Marinelli et al., 2020).

All previous factors interacting with CBD could be a potentially useful therapeutic option to improve chemosensitivity and cytotoxic effects on cancer cells and reduce cancer spread ,(Marinelli et al., 2020). Previous studies have shown that CBD has a very complex mechanism of action as an anti-cancer agent (Heider et al., 2022). However, despite a large number of *in vivo* and *in vitro* studies, there is still a need for more research to prove that CBD is synthesized and tested as a powerful drug that safely treats different types of human cancer (Massi et al., 2013). As shown in the Fig. 1, CBD has a very complex mechanism of action as an anti-cancer agent that safely treats different types of human cancer.

The current study pinpoints the interaction of cannabidiol (CBD) with the receptors responsible for anti-tumor action based on theoretical methods using the density function theory (DFT), molecular docking, and *in silico* ADMET proprieties. The optimized geometries were achieved by DFT method. The reactivity calculations predicted the interactions in the ligand-protein complex and their molecular boundary orbital analysis sites, which helped obtain the best molecular docking results. ADME/toxicity study was conducted to predict the bioavailability of cannabidiol.

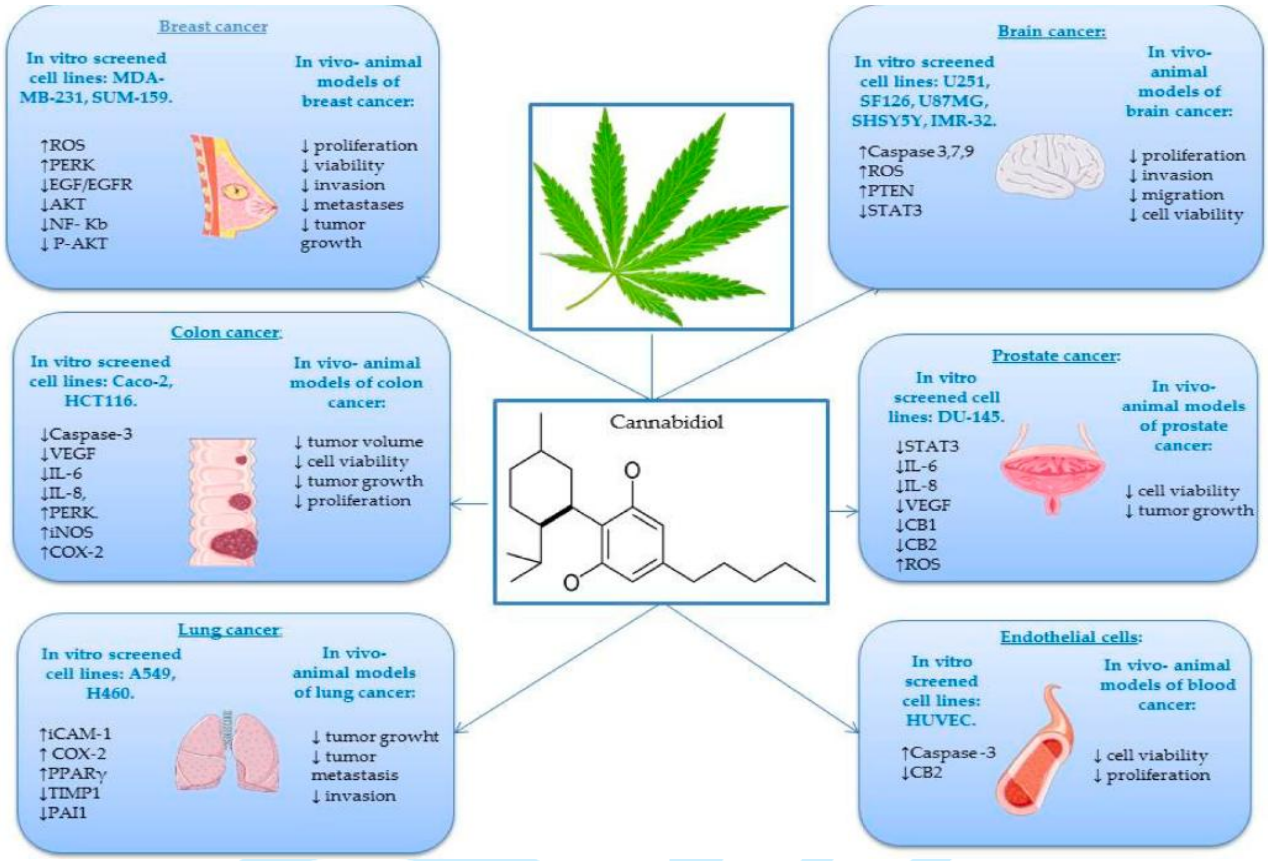

Fig. 1 Role of CBD among various cancer models (Kis et al., 2019)

2. Material and Methods

2.1 Density function theory (DFT) calculation

Gaussian 09 and GaussView 5 (Frisch et al., 2009) were used to calculate the optimal geometrical parameters of the target molecules using the density functional theory (DFT) approach at the B3LYP/6-31G++ level with Gaussian 09 and GaussView 5.

In this approach, the B3LYP functional, a hybrid functional combining the three-parameter Becke exchange (B3) and Lee-Yang-Parr correlation (LYP) functions, was used to determine the properties of cannabidiol and its electronic structure, based on 6-31G++ The molecules were imported into Gaussian 09 via GaussView 5.

The software then performed energy optimization calculations, where atom positions were adjusted to find the most stable configuration. These calculations provide geometrical information such as bond lengths and indications of electronic properties, such as the most stable and least energetic configuration, the energies of the frontier orbitals. The most occupied molecular orbital (HOMO) and the least occupied molecular orbital (LUMO) - and other parameters generated from these two energies and the molecular electrostatic potential (MESP).

2.2 Docking Molecular

2.2.1 Protein preparation

The cancer target proteins were downloaded in "pdb" format from the RCSB Protein Data Bank (PDB) database (https://www.rcsb.org) and were visualized using BIOVIA Discovery Studio (Tabti et al., 2023). Then, the protein was prepared and saved in PDBQT format in AutoDock workspace 4.2.6, in which polar hydrogen atoms and Kollman and Gasteiger charges were added for the protein (Trott & Olson, 2010). Table 1 displays the types of target studies, along with their corresponding PDB codes and the type of binding with the molecule

Table 1 Overview of proteins used

Receptor type	Pdb ID	Bound ligand
5-HT1A	7 e2z	Antagonist
Becl1	3q8t	Activator
CB1	5tgz	Antagonist
CB2	2hff	Inverse agonist
COX-2	1pxx	Inhibitor
DR5	4i9x	Against
EGF	1ivo	Agonist
FAAH	2wap	Inhibitor
GPR55	4n6h	Antagonist
ICAM-1	1iam	Activator
NOS3	1m7z	Inhibitor
NOXA	3mqp	Activator
PAI-1	7aqf	Inhibitor
PERK	4g31	Inducer
PPARɣ	5ycp	Agonist
TIMP-1	1d2b	Inhibitor
TRV1	7lqz	Agonist
TRV2	6u8a	Agonist

2.2.2 Ligands preparation

The DFT-optimized structure of cannabidiol (CBD) was imported and prepared in AutoDock workspace 4.2.6 for molecular docking simulation. Ligand preparation involves converting the ligand into the PDBQT format specifically required by AutoDock for docking. This format contains crucial information such as the partial charges and atom types required for accurate docking simulation

2.2.3 Visualization of protein-ligand interaction

The Autogrid algorithm in MGL Tools 1.5.6 was used to determine the potential size of the binding pocket between the receptor and cannabidiol. By setting the parameters to 8 binding modes and a completeness of 8, grid maps were generated using a size of 40 Å in all Cartesian directions. The binding pocket was defined using XYZ coordinates. Computational docking was performed with AutoDockVina software, and the Biovia Discovery Studio viewer was used to analyze docked conformations on the basis of established interactions (Dassault Systèmes BIOVIA, 2015).

Table 2 Overview of (XYZ) grid center coordinates used

Pdb ID	X	y	Z
7 e2z	93.694	73.002	87.111
3q8t	-59.211	-19.557	42.039
5tgz	43.637	27.469	318.530
2hff	-11.690	21.446	9.996
1pxx	69.156	36.960	34.659
4i9x	-4.491	12.415	48.441
1ivo	43.302	54.846	66.402
2wap	-6.748	27.359	37.499
4n6h	-5.910	69.366	70.805
1iam	37.909	79.263	12.440
1m7z	5.2869	43.300	13.035
3mqp	9.957	17.951	1.294
7aqf	34.166	9.525	23.511
4g31	-33.089	8.808	1.401
5ycp	35.1820	32.288	11.502
1d2b	-11.129	1.782	2.940
7lqz	170.831	105.917	107.590
6u8a	160.968	142.496	172.069

2.2.4 Physiochemical and pharmacokinetic evaluation

Prediction of the pharmacokinetic properties of cannabidiol is essential to determine the absorption, distribution, metabolism, excretion, and Toxicity of the active candidates molecules currently being studied for potential cancer treatment, and it was done using SwissADME (http://www.swissadme.ch/)

3. Results and Discussion

3.1 Optimized molecular geometry

Experimental information about the geometric properties of cannabidiol is insufficient in the literature. Theoretical calculation of the geometrical parameters of cannabidiol before optimization by DFT methods shows that cannabidiol has rings with an average C-C bond length of 1.550 Å, while the average C=C bond length is 1.386 Å where the typical C=C bond length is 1.346 Å and the typical distances between the C-C and C-H atoms for the substituted methyl are 1.519 Å and 1.110Å, respectively. The H-C-H angle of the methyl group is approximately 109°, and the alkene creates an angle with the neighboring carbon of about 123° of sp3 hybrid carbon forms an angle of about 120° with the C-C-C in the aromatic ring .When comparing the results in Table 3 with the CBD binding lengths before optimization by DFT, there is no difference.

Table 3 Calculated bond lengths of cannabinol molecule using DFT calculation

Bond lengths (Å)					
C1-C6	1.384	C11-C12	1.531	C17-C18	1.528
C1-O1	1.360	O7-H28	1.012	C18-H44	1.111
C1-C2	1.386	08-H29	1.012	C18-H45	1.111
C2-C14	1.536	C12-H36	1.111	C18-C19	1.526
C2-C3	1.389	C12-H37	1.111	C19-H25	1.115
C3-08	1.360	C12-C13	1.530	C19-C21	1.522
C3-C4	1.387	C13-H40	1.111	C21-C22	1.510
C4-H26	1.111	C13-H38	1.111	C21-C20	1.342
C4-C5	1.386	C13-H39	1.111	C20-H46	1.111
C5-C6	1.386	C14-H24	1.114	C20-H47	1.111
C5-C9	1.519	C14-C19	1.550	C22-H49	1.111
C9-H31	1.111	C14-C15	1.531	C22-H48	1.111
C9-H30	1.111	C15-C16	1.346	C22-H50	1.111
C9-C10	1.535	C15-H41	1.111	C23-H53	1.111
C10-H32	1.111	C16-C23	1.509	C23-H51	1.111
C10-H33	1.111	C16-C17	1.519	C23-H52	1.111
C10-H35	1.111	C17-H42	1.111		
C11-H34	1.111	C17-H43	1.111		

The cannabinol CBD molecule includes two rings; metabenzenediol and cyclohexene (Fig. 2). The chemical activity of cannabidiol (CBD) could result from the attachment of the hydroxyl radical teams to the C-1 and C-3 atoms of the benzene. Similarly, the alkyl radical fixed to the C-16 atom of the cyclohexene and pentyl to the C-5 atom of the aromatic ring can also contribute to the reactional activity of the molecule considered.

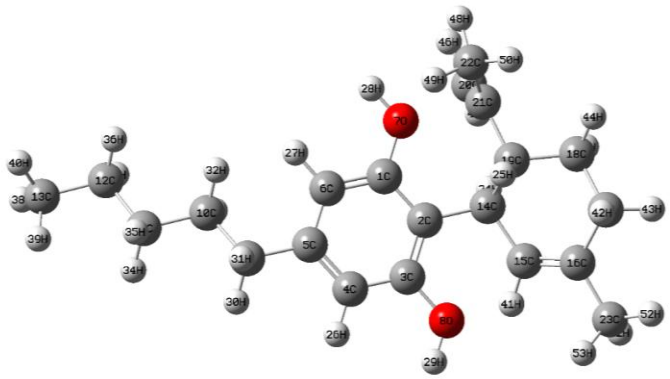

Fig. 2 Optimized geometry of cannabidiol optimized at the DFT/B3LYP/6-311++G(d.p) level

3.2 Frontier molecular orbital analysis HOMO-LUMO

HOMO and LUMO energies provide kinetic stability chemical analysis and band gap approximation (Fukui, 1982)

Table 4 Reports the values of the global molecular descriptors calculated for cannabidiol

$E_{(LUMO)}$ (eV)	$E_{(HOMO)}$ (eV)	ΔE (eV)	IP (eV)	EA (eV)	η (eV)	χ (eV)	ω (eV)	σ (eV)
0.012	-0.134	0.146	-0.012	0.134	0.073	0.060	0.0251	13.63

Equations (1-7) used to calculate the following quantum mechanical descriptors:
Electrophilicity index (ω), Chemical softness (σ) and hardness (η), Electronegativity (χ), Electronic affinity (EA), Ionization potential (IP) (Adjissi et al., 2022).

Energy gap (ΔE_{GAP} (eV))	$\Delta E = E_{LUMO} - E_{HOMO}$	(1)	Chemical softness (eV)	$\sigma = \frac{1}{\eta}$	(5)
Electronic affinity (eV)	$EA = -E_{LUMO}$	(2)	Electronegativity (eV)	$\chi = \frac{(IP + EA)}{2}$	(6)
Ionization potential (eV)	$IP = -E_{HOMO}$	(3)	Electrophilicity index ω (eV)	$\omega = \frac{\chi 2}{2\eta}$	(7)
Chemical hardness (eV)	$\eta = \frac{\Delta E}{2}$	(4)			

As shown in the Table 3 calculating the band gap energy E and the negative molecular chemical potential value of the cannabidiol molecule confirms that the molecule has a stable structure. A higher nucleophilic reactivity is indicated by the lower value of the electronic affinity and electrophilicity index (De Vleeschouwer et al., 2007). The higher values of durability and lower values of softness confirm that the durability of the molecule is higher and stability is one of the main characteristics of molecules that can be very reactive agents in anti-cancer activity. The first feature found is that LUMO is located on the π and π* orbitals of the benzene ring and HOMO is on the methyl group structure as shown in Fig. 3.

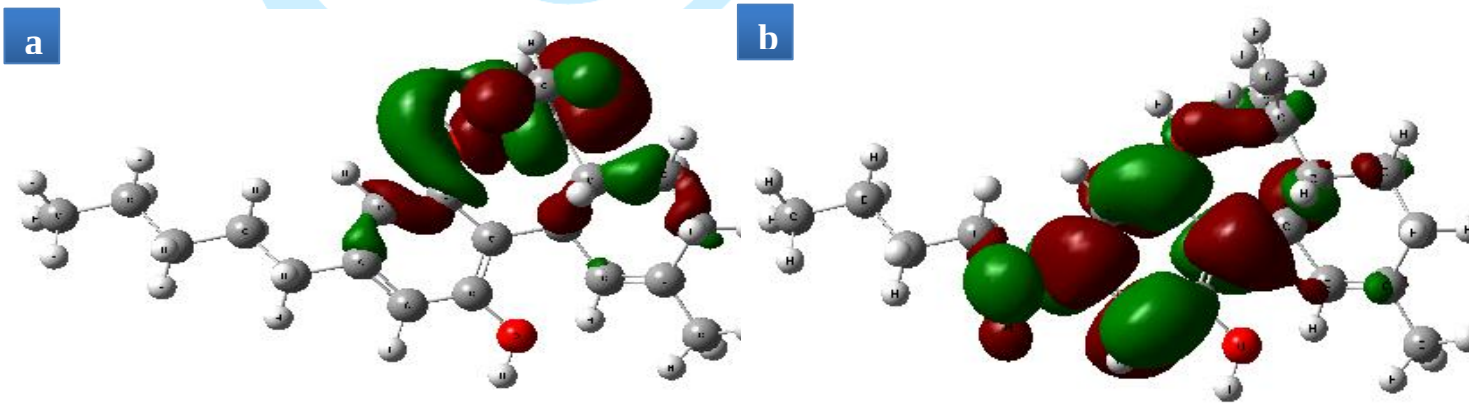

Fig. 3 HOMO (a) and LUMO (b) representation of CBD by DFT/ 631G method

3.3 Molecular Electrostatic Potential (MEP)

The interaction energy between the positive test charge of the molecular system and its charge distribution is known as the molecular electrostatic potential (MEP). It provides essential details on the chemical stability and reactivity of a semi-organic molecule allowing us to understand its electrophilic and nucleophilic properties.

Fig. 4 shows a color scale from red (negative MEP) through white (neutral MEP) to blue (positive MEP). Where blue regions indicate a vulnerable site for an electrostatic-type nucleophilic attack and red regions are sites for an electrostatic-type electrophilic attack (Leboeuf et al., 1999).

The negative electrostatic potential (region colored in red) was observed around the carbon atoms of the phenolic ring of the oxygen atom group. And the positive electrostatic potential (region colored in blue) was observed around the methyl group and the hydrogen atoms; this is due to the electronegative oxygen atom attracting electrons from the hydrogen atoms.

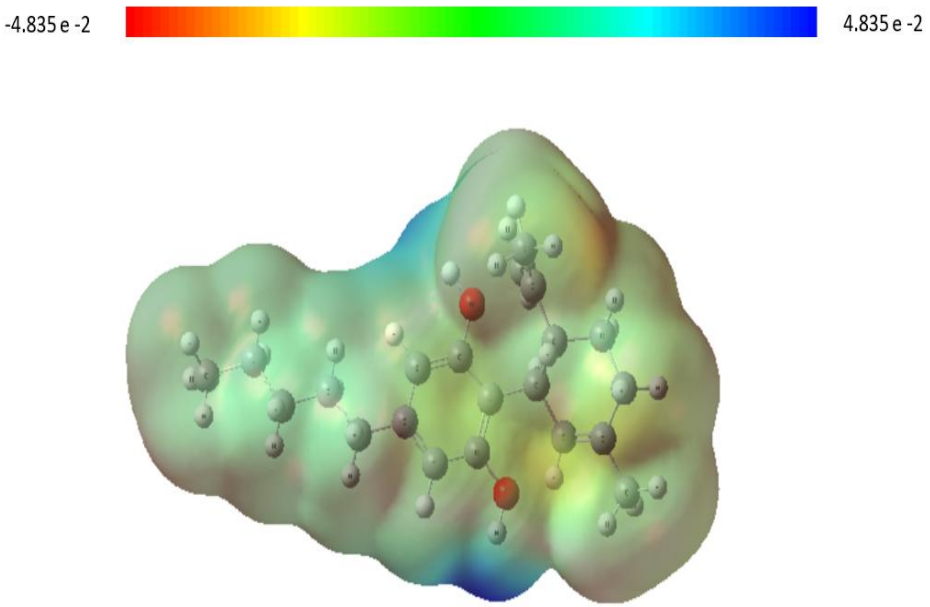

Fig. 4 Molecular electrostatic potential (MEP) surface of the cannabidiol (CBD) molecule

3.4 Molecular docking

3.4.1 Binding to 5-HT1A

Imidazole 5-HT1A showed an affinity of -7.4(kcal/mol) with CBD. As illustrated in Fig. 5(a) where hydroxyl group formed a hydrogen bond with the oxygen of amino acids SER316 and MET188 with distances of 2.408Å and 2.253 Å respectively. A pi-alkyl interaction between the carbon of the pentyl group and the Imidazole of HIS213 at 5.467 Å, while an alkyl, interaction was observed for cyclohexenyl group with ALA60 at 5.052 Å.

3.4.2 Binding to Becl1

Fig. 5(c) shows the interaction between CBD and Becl1 with a binding affinity of -5.5 kcal/mol. The hydrogen bond interaction were formed at the carbonyl group of amino acid ALA215 at 2.167 Å . In contrast. a carbon-hydrogen bond was formed between the oxygen of the hydroxyl group and the carbon of ARG219 at 3.692 Å. A pi-sigma bond was observed at 3.846 Å between the benzene ring and the methyl group of ALA215. Six alkyl interactions were found between the isopropyl group of ARG219 and cyclohexenyl group of CBD at 4.127 Å and cyclohexene at 4.925 Å. And between the pentyl carbon and LEU220 (5.470 Å), LYS212 (5.051 Å), and VAL213 (4.270 Å).

3.4.3 Binding to CB1

The binding energy between CBD and CB1 is -6.5 (kcal/mol) due to hydrogen bonding interaction observed at the hydroxyl group of cannabidiol with the oxygen of SER123 at 2.115 Å and ten alkyl bonding between cannabidiol and (MET103 at 4.976Å), (MET103 at 4.384 Å), (MET384 at 5.108 Å), (ILE119 at 4.353 Å), (MET384 at 4.288 Å), and Pi-Alkyl interaction with (PHE170 at 5.011 Å), (PHE381 at 5.019 Å), (ALA380 at 5.016 Å), (MET384 at 4.814 Å) as illustrated in Fig. 5(e).

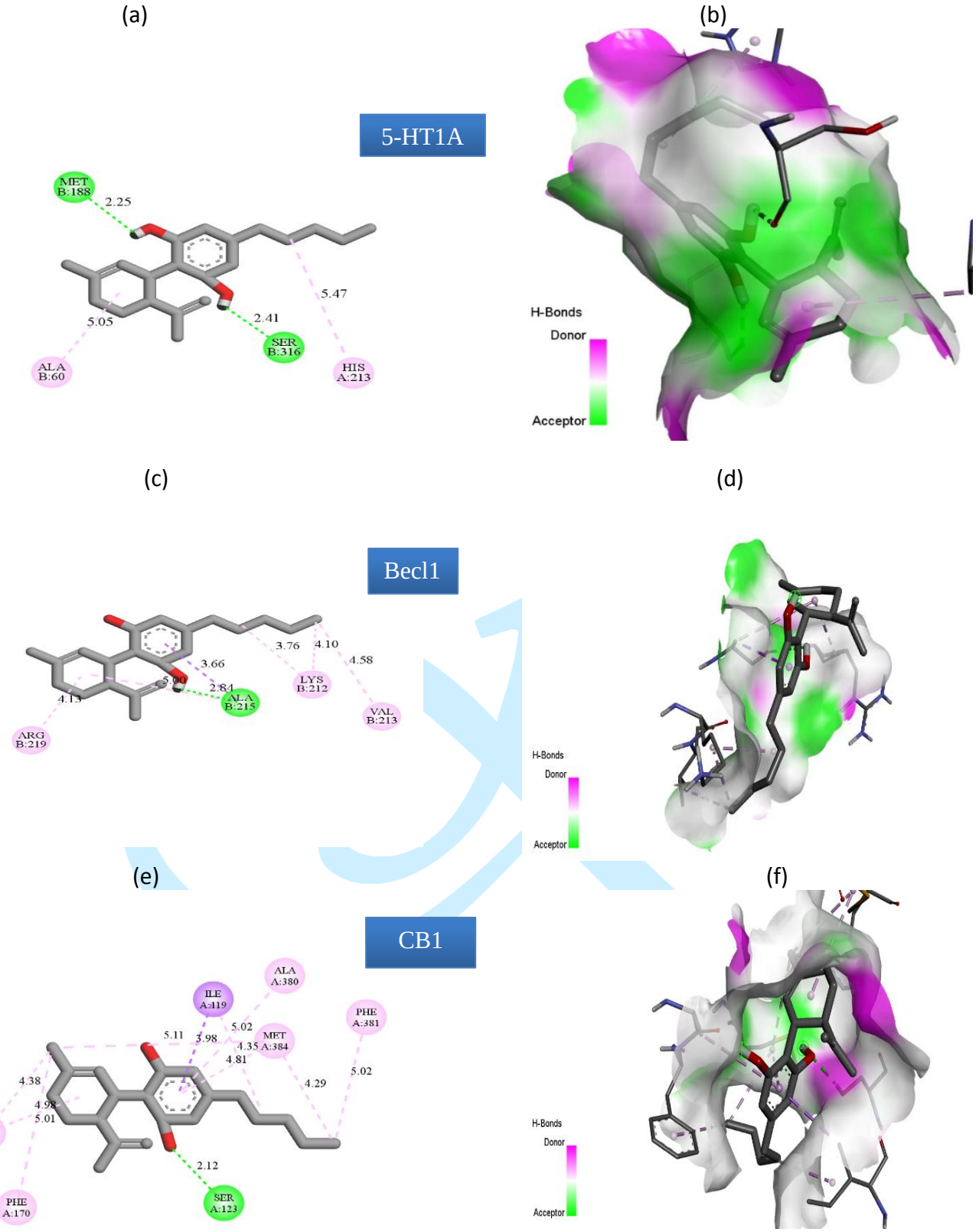

Interactions

Conventional hydrogen Bond

Alkyl

Pi-Sigma

Pi-Alkyl

Fig. 5 3D and 2D docked views of CBD with proteins 5-HT1A(b,a), Becl1 (d,c), and CB1(f,e)

3.4.4 Binding to CB2

CBD shows binding with CB2 with a binding energy of -6.8 (kcal/mol) due to the binding affinity between CB2 and CBD is -6.8 (kcal/mol). The hydroxyl group of CBD forms hydrogen bonds with CB2 and the hydrogen of the amine group of GLU212 at 2.351 Å and the oxygen of PRO119 at 2.073 Å. A Pi-Anion interaction at 2.073 Å between the benzene of CBD and PRO119. In addition, two alkyl bonds exist between (PRO118 at 4.152 Å), (ARG210 at 4.796 Å), and the carbon of CBD. Two pi-alkyl interactions between the benzene of CBD and ARG210 at 4.834 Å and the benzene PHE208 with the carbon of the methyl group CBD at 4.927 Å. And the Pi-Donor Hydrogen Bond with GLY211 at 3.19439 Å as illustrated in Fig. 6(a).

3.4.5 Binding to COX-2

The binding affinity of CBD with COX-2 is -8.0 (kcal/mol) due to three hydrogen interactions; two created by oxygen from the hydroxyl group with (CYS1047 at 2.266 Å) and (GLN1461 at 2.543 Å) and one form by hydrogen with oxygen from the amino acid (CYS1047 at 2.266 Å). Also, CBD makes a pi bond with COX-2 according to the Pi-alkyl bond with (PRO1153 at 4.503 Å) and alkyl interactions with the following amino acids (CYS1159 at 4.580 Å), (VAL1155 at 3.715 Å), (LYS1468 at 4.800 Å), (PRO1153 at 4.481 Å), and (LEU1152 at 5.266 Å) as illustrated in Fig. 6(c).

3.4.6 Binding to DR5

The binding affinity between DR5 and CBD is -8.2 (kcal/mol) because CBD makes one hydrogen bond THR68 at 2.222 Å and the hydrogen of the hydroxyl group. Also, it makes four pi-alkyl bonds with (PHE157 at 4.905 Å), (TYR181 at 4.41 Å), (TRP188 with two interactions at 5.056Å and at 4.906 Å) and (PRO52 at 4.895Å), while four alkyl bonds are formed with (PRO52 at 4.811 Å), (ALA44 at 4.863Å), (ALA44 at 3.602 Å), (PRO52 at 4.696 Å), (LEU123 at 3.911 Å). The Pi-Pi Stacked interaction has 4.740Å between the benzene of CBD and that of TYR181 as illustrated in Fig. 6(e).

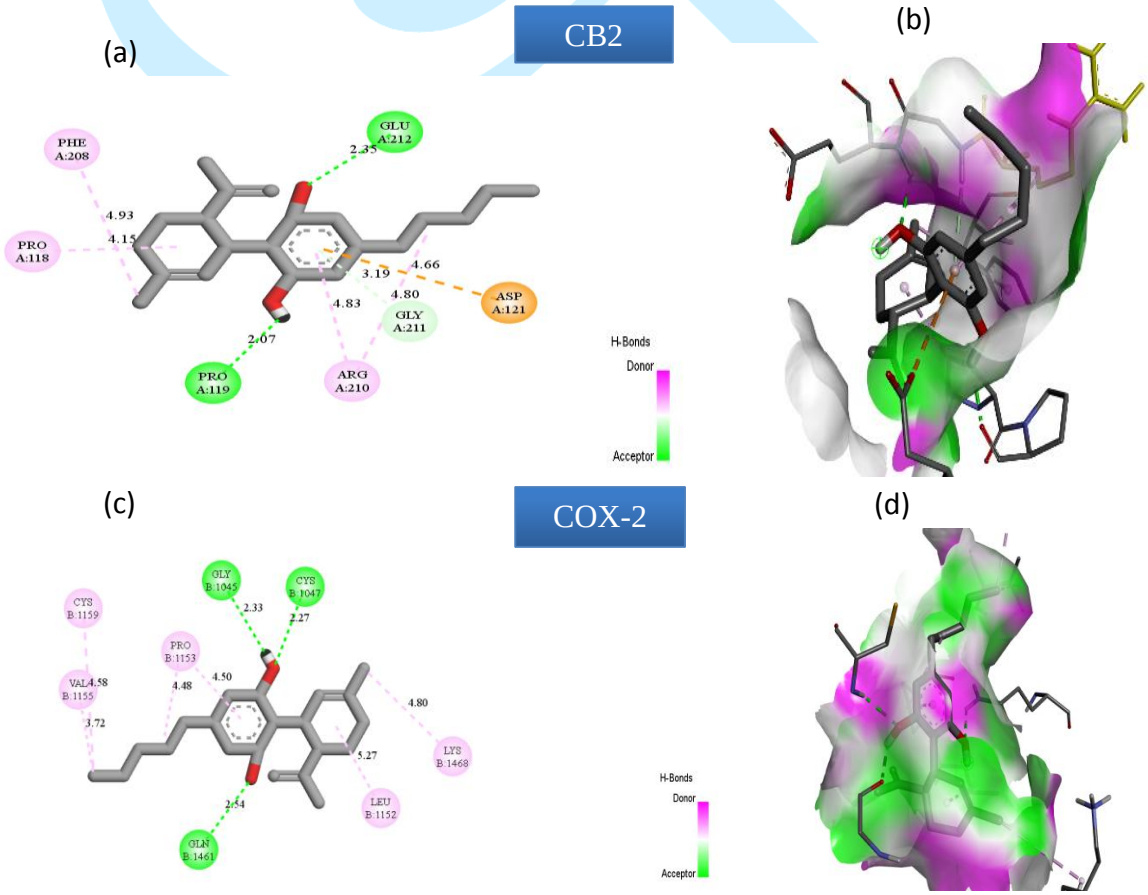

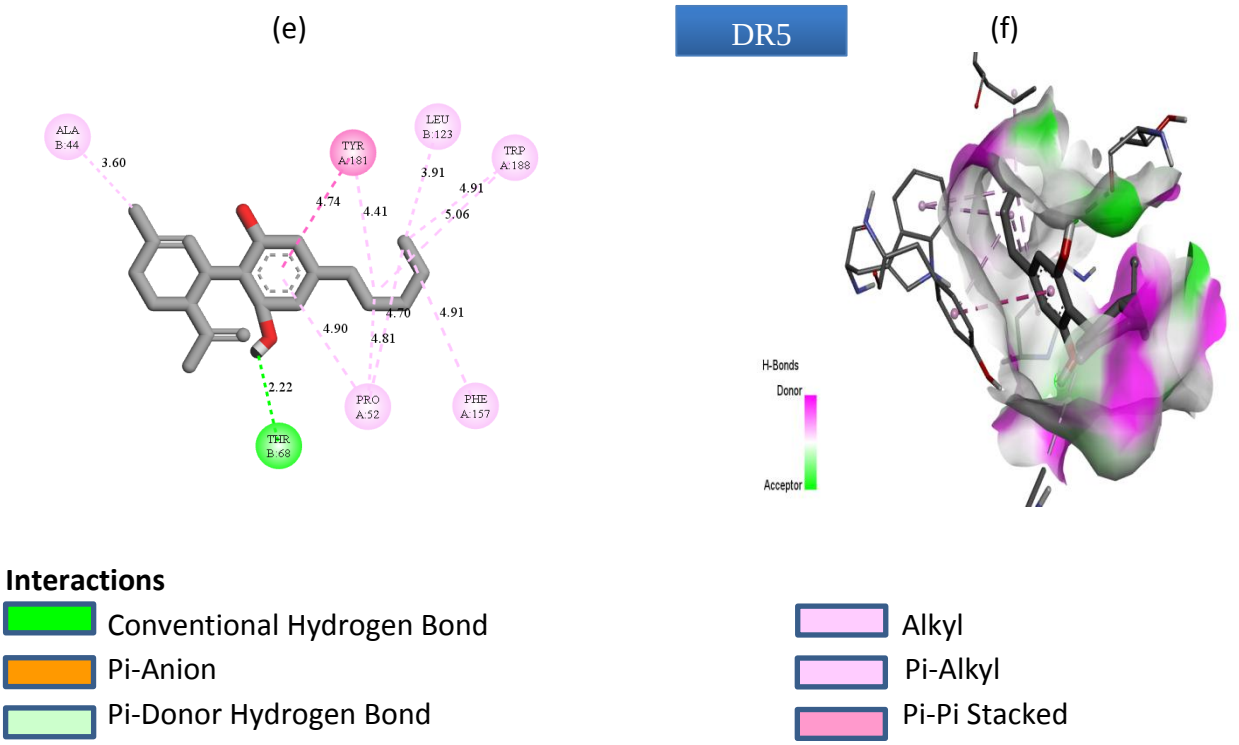

Fig. 6 3D and 2D docked views of CBD with Proteins CB2 (b,a),COX-2(d,c), and DR5(f,e)

3.4.7 Binding to EGF

The binding affinity between EGF and CBD is with EGF of -7.5 (kcal/mol) because CBD makes hydrogen bonding with (SER11 at 2.963Å), (HIS409 at 2.241Å), and (GLY9 at 1.99Å. and five alkyl type interaction with the following amino acids (LYS48 at 4.955Å), (MET30 at 5.147Å), (ILE38 at 5.055Å), (MET30 at 4.302Å), (LYS48 at 4.361 Å). Also four pi-alkyl bond was formed (HIS409 at 4.681Å), (TRP49 at 5.278Å), (TRP49 at 4.470Å), (ILE38 at 4.971 Å), Fig. 7(a).

3.4.8 Binding to FAAH

The binding affinity between FAAH and CBD is -8.6 (kcal/mol) because CBD makes one Pi-Pi T-shaped interaction with (PHE432 at 5.305Å), and four Alkyl interactions with (LEU404 at 5.141Å), (VAL491 at 5.077Å), (LEU404 at 3.977Å), (MET495 at 5.456 Å). In addition, four Pi-Alkyl bond with (PHE432 at 4.977Å), (PHE432 at 4.730 Å), (TRP531 at 5.054Å), (VAL491 at 4.380 Å), Fig. 7(c).

3.4.9 Binding to GPR55

The binding affinity between GPR55 and CBD is -7.0 (kcal/mol) because CBD makes two hydrogen bond (TYR308 at 2.031Å), (ASP128 at 2.685Å). One Pi-Sigma bond (ILE304 at 3.901Å), two Alkyl bond with (ILE277 at 3.953Å), and (ILE304 at 4.661Å), and two Pi-Alkyl bond with (TRP274 at 4.784Å), (HIS301 at 4.620 Å) Fig. 7(e).

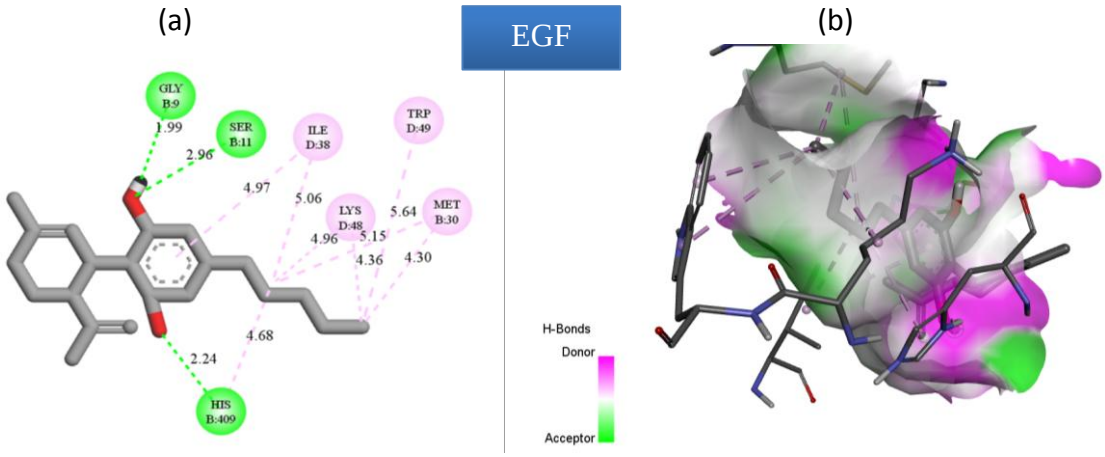

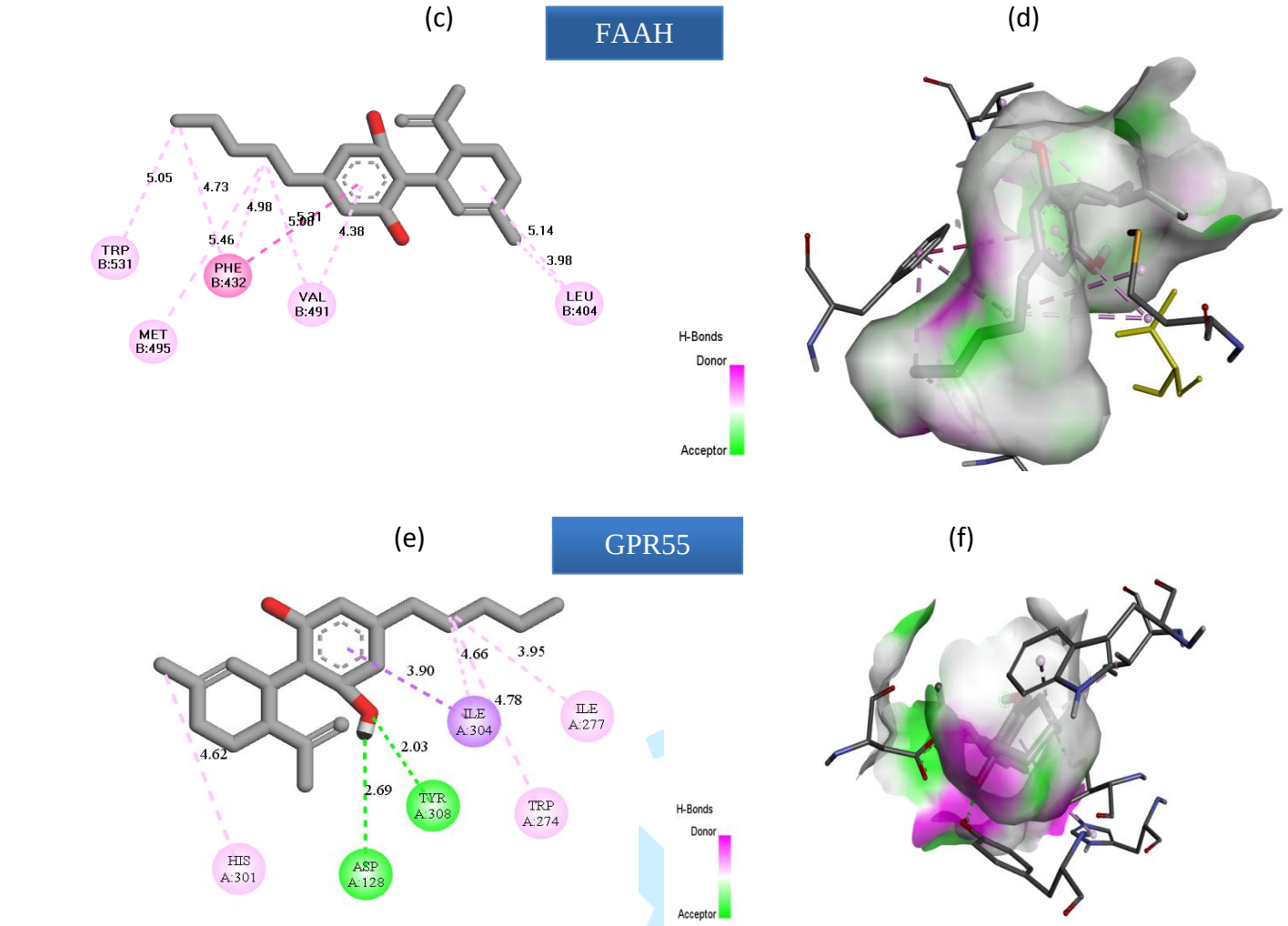

Fig. 7 3D and 2D docked views of CBD with Proteins EGF(b,a), FAAH(d,c) and GPR55(f,e)

3.4.10 Binding to ICAM-1

The binding affinity between ICAM-1 and CBD is -5.2 (kcal/mol) because CBD makes one hydrogen bonds (LEU94 at 2.702Å), while a Pi-Pi T-shaped bond forms between the benzene of CBD and (TYR180 at 5.154 Å) with one alkyl bonds (PRO93 at 5.119 Å) (Fig. 8a).

3.4.11 Binding to NOS3

The binding affinity between NOS3 and CBD is -7.0 (kcal/mol) because CBD forms hydrogen bonds with NOS3 (GLY233 at 2.405 Å) and a Pi-Anion interaction at 4.01736 Å between the benzene of CBD and GLU239. In addition, two alkyl bonds exist between (CYS62 at 4.540Å), (ILE214 at 5.228 Å), and the carbon of CBD. Seven pi-alkyl interactions occur between the benzene groups of CBD and (PRO212 at 5.177Å).(ILE214 at 5.42443) and the benzene rings of TRP56, PHE231 and TYR235 with the carbon of the group CBD at 5.167 Å. 5.220 Å and 5.351 Å respectively (Fig. 8c).

3.4.12 Binding to NOXA

The binding affinity between NOXA and CBD is - -5.7 (kcal/mol) because CBD forms hydrogen bonds with NOXA (LYS101 has 2.496Å), and a single pi-anion was observed towards (GLU49 has 4.863 Å), and a Pi-cation

with LYS101 at 4.101Å, and Pi-Sigma with at 3.94 Å, a pi-alkyl bond with YS101 at 4.704 Å respectively. Seven alkyl interaction with (LYS53 at 5.295Å), (LYS101 at 5.241Å), (ARG105 at 4.764Å), (LYS101 at 4.322 Å), (LEU104 at 4.315Å), (LEU56 at 4.364Å), and (ILE98 at 5.387Å) (Fig. 8e).

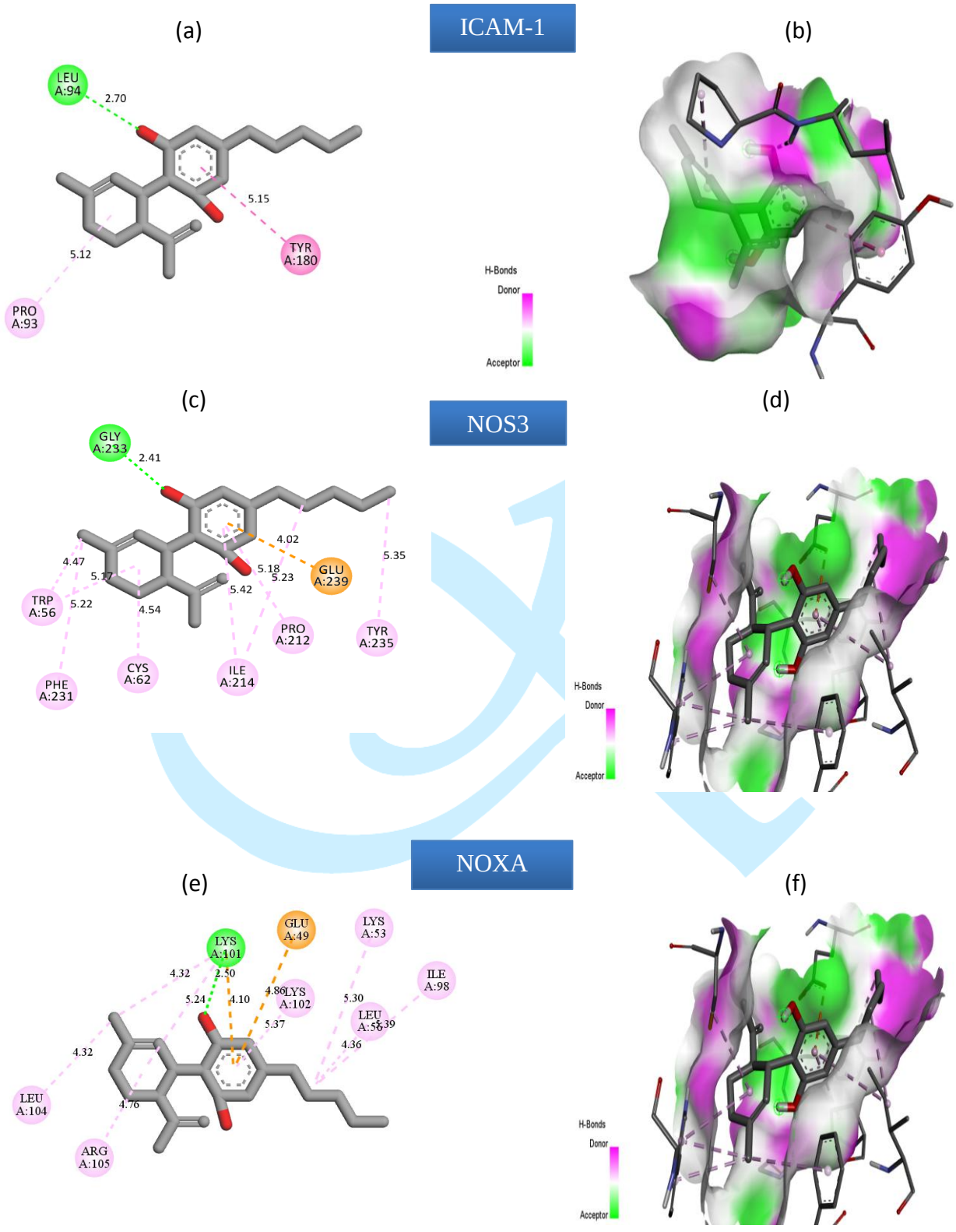

Interactions

- Conventional Hydrogen Bond
- Pi-Anion
- Pi-Pi-T- Stacked
- Alkyl
- Pi-Alkyl

Fig. 8 3D and 2D docked views of CBD with Proteins ICAM-1(b,a),NOS3(d,c), and NOXA(f,e)

3.4.13 Binding to PAI-1

The interaction between CBD and PAI-1 has a binding energy of -8.0 kcal/mol; CBD forms one hydrogen bond with (GLU281 at 2.281 Å) and (GLU281: O a 1.99567 Å). Also, one Pi-Sigma bond with (THR282 at 3.768Å), and six alkyl bonds with VAL23 a 5.297Å, VAL32 at 5.271 Å, VAL284 at 5.443Å, LEU152 at LEU152 at 4.362Å and VAL23 at 4.488 Å, VAL284 at 4.291Å (Fig. 9a)

3.4.14 Binding to PERK

The interaction between CBD and PERK has a binding energy of -7.0 kcal/mol; CBD forms two hydrogen bond with ASN941 and LEU598 at 1.9138 Å, 2.477Å respectively, a pi-sigma bond with PHE943 at 3.685Å. Also, T-shaped Pi-Pi formed with the amino acids PHE943 at 4.836 Å. In addition, two alkyl bonds (VAL606 at 4.872Å), (ALA619 at 4.014Å) two interaction (PHE943 at 5.180 Å), (VAL606 at 4.246 Å) (Fig. 9c)

3.4.15 Binding to PPARɣ

The interaction between CBD and PPARɣ TIMP-1 has a binding energy of -6.3 kcal/mol. It forms one carbon hydrogen bond GLY284 with at 3.487 Å. One Pi-Sulfur interaction with MET348 at 5.129Å. Also, four alkyl interactions with CYS285 at 4.417Å and ARG288 at 4.606 Å. ARG280 at 3.659 Å and ILE341at 4.749 Å. While CBD makes one pi-alkyl interactions with ILE341 at 4.497Å (Fig. 9e).

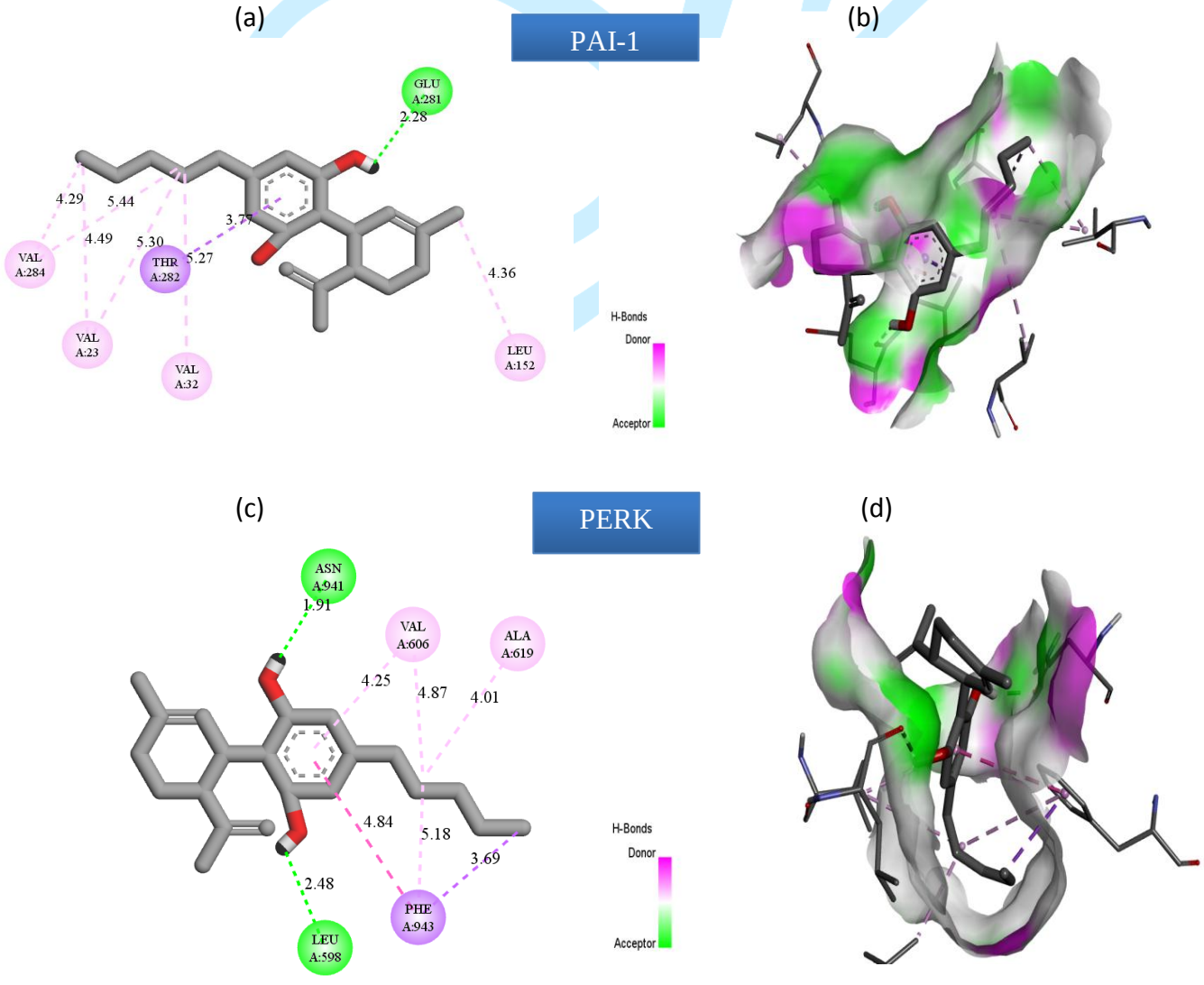

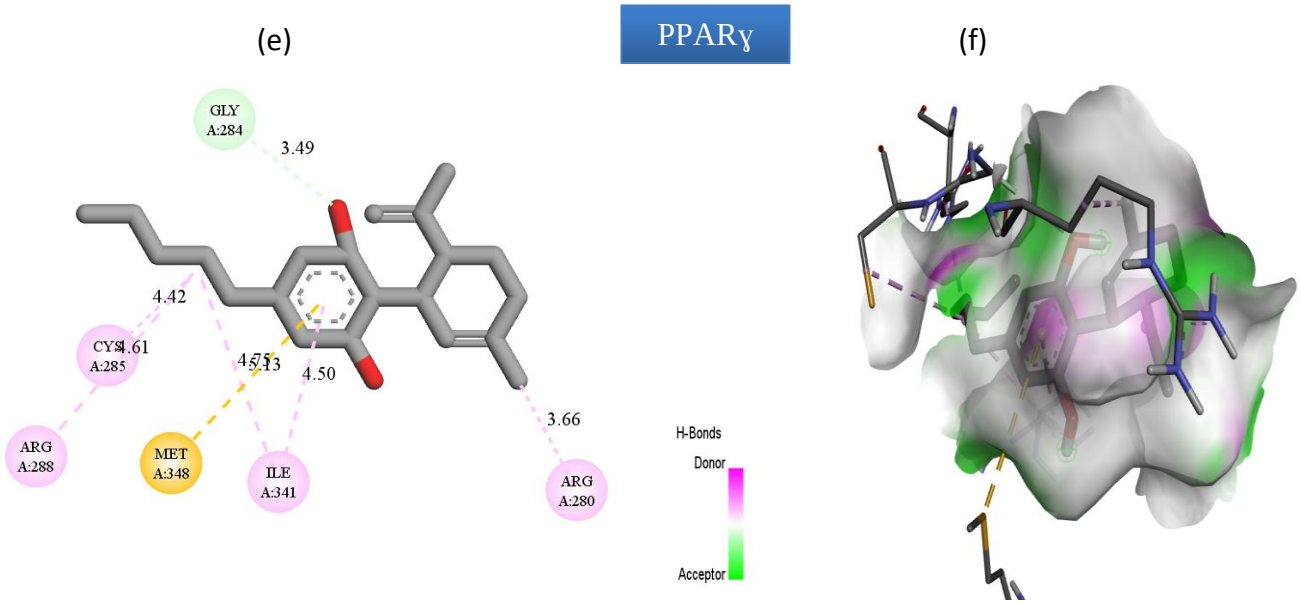

Fig. 9 3D and 2D docked views of cbd with Proteins PAI-1(b,a),PERK(d,c), and PPARɣ (f,e)

3.4.16 Binding to TIMP-1

The interaction between CBD and TIMP-1 has a binding energy of -6.7 kcal/mol. It forms one hydrogen bond SER100 with at 2.686. A Pi-Donor Hydrogen Bond interaction with VAL102 at 5.129Å. Also, four Pi-Alkyl interactions with TYR72 at 4.108Å and PHE101 at 3.911Å. PRO5 at 4.248Å and ALA103 at 4.610 Å. While CBD makes two alkyl interactions with PRO5 and ALA103 at 4.802Å and 4.389 Å (Fig. 10a).

3.4.17 Binding to TRV1

The interaction between CBD and TRV1 has a binding energy of -7.1 kcal/mol. It forms a conventional hydrogen bond interaction with VAL449 at 2.123 Å. A carbon hydrogen bond with GLY479 at 3.506 Å. A Pi-Sigma interaction with THR452 and TYR456 at 3.955 Å and 3.789 Å respectively .Two pi-alkyl with TYR456 at 4.782 Å and ALA453 at 5.061 Å. Furthermore, seven alkyl interactions (VAL449 at 4.322 Å), (ARG476 at 4.328 Å), (ILE448 at 5.056Å) were observed (Fig. 10c).

3.4.18 Binding to TRV2

The interaction between CBD and TRV2 has a binding energy of -7.1 kcal/mol. It forms one conventional hydrogen bond with VAL449 at 2.123 Å. In addition, it forms three hydrophobic bonds of alkyl type (VAL449 at 4.329Å). (ARG476 at 4.328Å), and (4.328 at 5.056Å), and two pi-alkyl interactions with (PHE540 a 5.43731 Å), (PHE540 a 4.54944 Å), (TYR544 a 4.10511 Å), (TYR456 at 4.782Å), (ALA453 at 5.061Å), and two Pi-Sigma with (THR452 at 3.9558 Å) and (A:TYR456 at 3.789Å) (Fig. 10e).

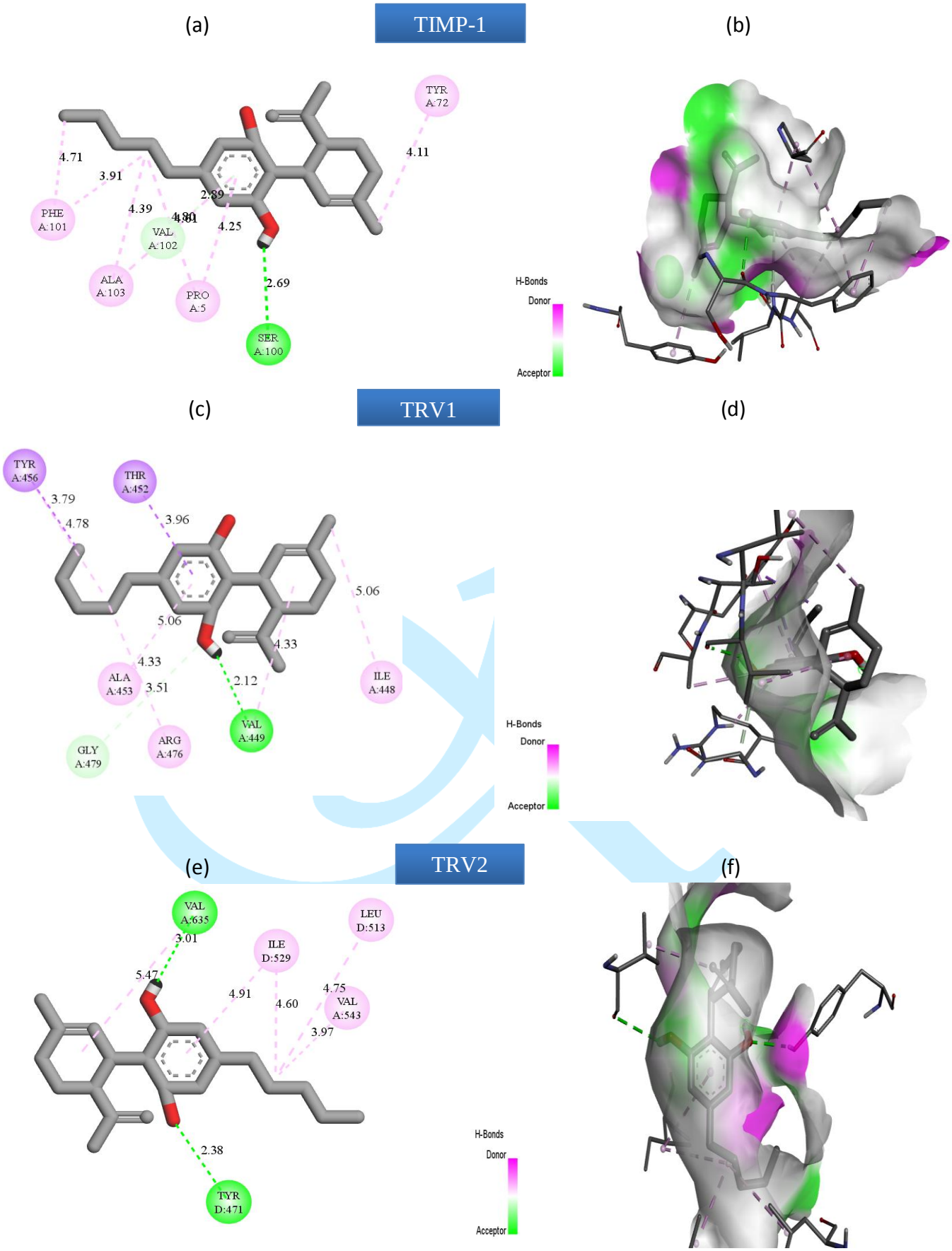

Interactions

- Conventional Hydrogen Bond
- Alkyl
- Pi-Sigma
- Pi-Alkyl
- Pi-Donor Hydrogen Bond
- Carbon Hydrogen Bond

Fig. 10 3D and 2D docked views of CBD with Proteins TIMP-1(b,a), TRV1(d,c),and TRV2(f,e)

3.5 ADMET proprieties

The ADMET property is an acronym used in pharmacology and drug development and standing for absorption, distribution, metabolism, excretion, and toxicity. These properties play a crucial role in determining the pharmacokinetics and potential therapeutic value of a compound. Table 5 presents the ADMET properties (absorption, distribution, metabolism, excretion, and toxicity) associated with the CBD under investigation. Providing valuable insights into its potential as a drug candidate

Table 5 Results of the ADMET test with pKCSM of CBD

Absorption	
Intestinal absorption (human)	**90.854** % Absorbed
Distribution	
BBB permeability	**0.181** log BB
CNS permeability	**-3.911** logPS
Metabolism	
CYP 2D6 Substrate	**No**
CYP 3A4 Substrate	**Yes**
CYP 2D6 Inhibitor	**No**
CYP3A4 Inhibitor	**No**
Excretion	
Renal Oct-02 substrate	**No**
Toxicity	
AMES	**No**
Hepatoxicity	**No**

Based on the results obtained in Table 4. CBD absorption by the human intestine is at 90.854%. Guaranteeing excellent absorption by the human intestine. However, regarding distribution indicators. The standard value of blood-brain barrier (BBB) permeability is good if its value is greater than 0.3 and poor if LogBB < -1. The results show that CBD responds well to the BBB criteria. which predicts that the drugs can pass through the brain. CNS index. The compound with LogPS > -2 is considered able to penetrate the CNS. And the compound with Log PS < -3 is considered unable to penetrate the CNS; therefore. cannabidiol can penetrate the CNS. CYP enzymes are enzymes that oxidize foreign microorganisms to facilitate their excretion. Inhibition of this enzyme can affect the drug's metabolism. And the drug can have a reverse effect through 2D6 and 3A4 inhibitors responsible for drug metabolism. According to the results. CBD can be considered a substrate of CYP3A4 but not a CYP inhibitor. Indicating that CBD's metabolism as a drug is acceptable. As for the toxicity requirement. CB has no potential harmful effect and does not cause hepatotoxicity.

Table 6 Results of the assessment of Cannabidiol (CBD) compliance with Lipinski's five rules

Molecular weight (g/mol)	LogP	H-bond acceptors	H-bond donors	Rotatable bonds
352.773	4.28	2	2	6

The analysis of the ADMET results (Table 6) and the Lipinski rules (MW<=500; logP<=5; Hacc<=10; Hdon<=5) indicate that the studied molecule has been verified *in silico* as a safe pharmaceutical compound.

4. Conclusion

The results of this study indicate that cannabidiol has the potential to be an effective tumor treatment. Analysis using the DFT method showed that the -OH groups present in cannabidiol create hydrogen bonding interactions with cancer site targets (5-HT1A, Becl1, COX-2, DR5, EGF, FAAH, ICAM-1, NOS3, NOXA, PAI-1,

PERK, RERK, TIMP-1 and TRV1/2). Resulting in a high binding energy (-8.6, -8.2, -8.0 kcal/mol respectively with FAAH, DR5, COX-2, and -8.2 kcal/mol with TRV1/2). As shown by molecular docking simulation, indicating that cannabidiol has considerable affinity for cancer site targets. These results are encouraging and suggest that cannabidiol may be a promising treatment for tumors. However, further studies are needed to determine the efficacy of cannabidiol in cancer treatment and to understand the exact molecular mechanisms involved in this anticancer activity.

Funding Information

This research did not receive any specific grant from funding agencies in the public, commercial, or not-for-profit sectors.

Declaration of Conflict

The authors declare that they have no known competing financial interests or personal relationships that could have appeared to influence the work reported in this paper.

References

1. Adjissi, L., Chafai, N., Benbouguerra, K., Kirouani, I., Hellal, A., Layaida, H., Elkolli, M., Bensouici, C., & Chafaa, S. (2022). Synthesis, characterization, DFT, antioxidant, antibacterial, pharmacokinetics and inhibition of SARS-CoV-2 main protease of some heterocyclic hydrazones. *Journal of Molecular* Structure, 1270, 134005. https://doi.org/10.1016/j.molstruc.2022.134005
2. Andradas, C., Truong, A., Byrne, J., & Endersby, R. (2021). The Role of Cannabinoids as Anticancer Agents in Pediatric Oncology. Cancers, 13(1), Article 1. https://doi.org/10.3390/cancers13010157
3. Atalay, S., Jarocka-Karpowicz, I., & Skrzydlewska, E. (2020). Antioxidative and Anti-Inflammatory Properties of Cannabidiol. *Antioxidants, 9*(1), Article 1. https://doi.org/10.3390/antiox9010021
4. Brand, E. J., & Zhao, Z. (2017). Cannabis in Chinese Medicine : Are Some Traditional Indications Referenced in Ancient Literature Related to Cannabinoids? *Frontiers in Pharmacology*, 8. https://www.frontiersin.org/article/10.3389/fphar.2017.00108
5. Brunetti, L., Loiodice, F., Piemontese, L., Tortorella, P., & Laghezza, A. (2019). New Approaches to Cancer Therapy : Combining Fatty Acid Amide Hydrolase (FAAH) Inhibition with Peroxisome Proliferator-Activated Receptors (PPARs) Activation: Miniperspective. *Journal of Medicinal Chemistry, 62*(24), 10995‑11003. https://doi.org/10.1021/acs.jmedchem.9b00885
6. Calvillo-Robledo, A., Cervantes-Villagrana, R. D., Morales, P., & Marichal-Cancino, B. A. (2022). The oncogenic lysophosphatidylinositol (LPI)/GPR55 signaling. *Life Sciences, 301*, 120596. https://doi.org/10.1016/j.lfs.2022.120596
7. Cannabidiol-induced apoptosis is mediated by activation of Noxa in human colorectal cancer cells | Lecteur amélioré Elsevier. (s. d.). https://doi.org/10.1016/j.canlet.2019.01.011
8. Clarke, R. C., & Merlin, M. D. (2015). Letter to the Editor : Small, Ernest. 2015. Evolution and Classification of Cannabis sativa (Marijuana, Hemp) in Relation to Human Utilization. Botanical Review. *The Botanical Review, 81*(4), 295‑305. https://doi.org/10.1007/s12229-015-9158-2
9. Corvino, A., Fiorino, F., Severino, B., Saccone, I., Frecentese, F., Perissutti, E., Di Vaio, P., Santagada, V., Caliendo, G., & Magli, E. (2018). The Role of 5-HT1A Receptor in Cancer as a New Opportunity in Medicinal Chemistry. *Current Medicinal Chemistry, 25*(27), 3214‑3227. https://doi.org/10.2174/0929867325666180209141650
10. Dassault Systèmes BIOVIA. (2015). Discovery studio modeling environment (Release 4). San Diego.
11. De Almeida, D. L., & Devi, L. A. (2020). Diversity of molecular targets and signaling pathways for CBD. *Pharmacology Research & Perspectives, 8*(6), e00682. https://doi.org/10.1002/prp2.682
12. De Vleeschouwer, F., Van Speybroeck, V., Waroquier, M., Geerlings, P., & De Proft, F. (2007). Electrophilicity and Nucleophilicity Index for Radicals. *Organic Letters, 9*(14), 2721‑2724. https://doi.org/10.1021/ol071038k

13. Drozd, M., Marzęda, P., Czarnota, J., Dobrzyński, M., Skubel, T., Dudek, I., & Rybak, N. (2022). The potential of cannabinoids in the treatment of lung cancer. *Journal of Education, Health and Sport, 12*(8), Article 8. https://doi.org/10.12775/JEHS.2022.12.08.094
14. Fan, P., & Jordan, V. C. (2022). PERK, Beyond an Unfolded Protein Response Sensor in Estrogen-Induced Apoptosis in Endocrine-Resistant Breast Cancer. *Molecular Cancer Research, 20*(2), 193‑201. https://doi.org/10.1158/1541-7786.MCR-21-0702
15. Frisch, M. J., Trucks, G. W., Schlegel, H. B., Scuseria, G. E., Robb, M. A., Cheeseman, J. R., ... & Fox, D. J. (2009). Gaussian 09, Revision A.02. Gaussian, Inc., Wallingford CT.
16. Fukui, K. (1982). Role of Frontier Orbitals in Chemical Reactions. *Science, 218*(4574), 747‑754. https://doi.org/10.1126/science.218.4574.747
17. Giatromanolaki, A., Koukourakis, M. I., Georgiou, I., Kouroupi, M., & Sivridis, E. (2018). LC3A, LC3B and Beclin-1 Expression in Gastric Cancer. *Anticancer Research, 38*(12), 6827‑6833. https://doi.org/10.21873/anticanres.13056
18. Hajji, H., Tabti, K., En-nahli, F., Bouamrane, S., Lakhlifi, T., Ajana, M., & Bouachrine, M. (2021). In Silico Investigation on the Beneficial Effects of Medicinal Plants on Diabetes and Obesity : Molecular Docking, Molecular Dynamic Simulations, and ADMET Studies. *Biointerface Research in Applied Chemistry, 11*, 6933‑6949. https://doi.org/10.33263/BRIAC115.69336949
19. He, X.-X., Shi, L.-L., Qiu, M.-J., Li, Q.-T., Wang, M.-M., Xiong, Z.-F., & Yang, S.-L. (2018). Molecularly targeted anti-cancer drugs inhibit the invasion and metastasis of hepatocellular carcinoma by regulating the expression of MMP and TIMP gene families. *Biochemical and Biophysical Research Communications, 504*(4), 878-884. https://doi.org/10.1016/j.bbrc.2018.08.203
20. Heider, C. G., Itenberg, S. A., Rao, J., Ma, H., & Wu, X. (2022). Mechanisms of Cannabidiol (CBD) in Cancer Treatment: A Review. *Biology, 11*(6), 817.
21. Hou, N., He, X., Yang, Y., Fu, J., Zhang, W., Guo, Z., Hu, Y., Liang, L., Xie, W., Xiong, H., Wang, K., & Pang, M. (2019). TRPV1 Induced Apoptosis of Colorectal Cancer Cells by Activating Calcineurin-NFAT2-p53 Signaling Pathway. *BioMed Research International, 2019*, e6712536. https://doi.org/10.1155/2019/6712536
22. Hou, Y.-J., Li, D., Wang, W., Mao, L., Fu, X., Sun, B., & Fan, C. (2022). NT157 inhibits cell proliferation and sensitizes glioma cells to TRAIL-induced apoptosis by up-regulating DR5 expression. *Biomedicine & Pharmacotherapy, 153*, 113502. https://doi.org/10.1016/j.biopha.2022.113502
23. Hou, Y.-J., Li, D., Wang, W., Mao, L., Fu, X., Sun, B., & Fan, C. (2022). NT157 inhibits cell proliferation and sensitizes glioma cells to TRAIL-induced apoptosis by up-regulating DR5 expression. *Biomedicine & Pharmacotherapy, 153*, 113502. https://doi.org/10.1016/j.biopha.2022.113502
24. Jeong, S., Kim, B. G., Kim, D. Y., Kim, B. R., Kim, J. L., Park, S. H., Na, Y. J., Jo, M. J., Yun, H. K., Jeong, Y. A., Kim, H. J., Lee, S. I., Kim, H. D., Kim, D. H., Oh, S. C., & Lee, D.-H. (2019). Cannabidiol Overcomes Oxaliplatin Resistance by Enhancing NOS3- and SOD2-Induced Autophagy in Human Colorectal Cancer Cells. *Cancers, 11*(6), Article 6. https://doi.org/10.3390/cancers11060781
25. Jeong, S., Yun, H. K., Jeong, Y. A., Jo, M. J., Kang, S. H., Kim, J. L., Kim, D. Y., Park, S. H., Kim, B. R., Na, Y. J., Lee, S. I., Kim, H. D., Kim, D. H., Oh, S. C., & Lee, D.-H. (2019). Cannabidiol-induced apoptosis is mediated by activation of Noxa in human colorectal cancer cells. *Cancer Letters, 447*, 12‑23. https://doi.org/10.1016/j.canlet.2019.01.011
26. Khunluck, T., Lertsuwan, K., Chutoe, C., Sooksawanwit, S., Inson, I., Teerapornpuntakit, J., Tohtong, R., & Charoenphandhu, N. (2022). Activation of cannabinoid receptors in breast cancer cells improves osteoblast viability in cancer-bone interaction model while reducing breast cancer cell survival and migration. *Scientific Reports, 12*(1), 7398. https://doi.org/10.1038/s41598-022-11116-9
27. Kis, B., Ifrim, F. C., Buda, V., Avram, S., Pavel, I. Z., Antal, D., Paunescu, V., Dehelean, C. A., Ardelean, F., Diaconeasa, Z., Soica, C., & Danciu, C. (2019). Cannabidiol—from Plant to Human Body : A Promising Bioactive Molecule with Multi-Target Effects in Cancer. *International Journal of Molecular Sciences, 20*(23), Article 23. https://doi.org/10.3390/ijms20235905

28. Lamdabsri, V., Buaban, K., Taechowisan, T., Phutdhawong, W. S., & Phutdhawong, W. (2021). Chemical composition of seized cannabis and its extraction for medical purposes. *Maejo Int. J. Sci. Technol.*, 11.
29. Leboeuf, M., Köster, A. M., Jug, K., & Salahub, D. R. (1999). Topological analysis of the molecular electrostatic potential. *The Journal of Chemical Physics, 111*(11), 4893‑4905. https://doi.org/10.1063/1.479749
30. Li, S., Jiang, M., Wang, L., & Yu, S. (2020). Combined chemotherapy with cyclooxygenase-2 (COX-2) inhibitors in treating human cancers: Recent advancement. *Biomedicine & Pharmacotherapy, 129*, 110389. https://doi.org/10.1016/j.biopha.2020.110389
31. Lichtor, T. (2015). Molecular Considerations and Evolving Surgical Management Issues in the Treatment of Patients with a Brain Tumor. BoD – Books on Demand.
32. Liu, S., Shi, J., Wang, L., Huang, Y., Zhao, B., Ding, H., Liu, Y., Wang, W., Chen, Z., & Yang, J. (2022). Loss of EMP1 promotes the metastasis of human bladder cancer cells by promoting migration and conferring resistance to ferroptosis through activation of PPAR gamma signaling. *Free Radical Biology and Medicine, 189*, 42-57. https://doi.org/10.1016/j.freeradbiomed.2022.06.247
33. Loss of EMP1 promotes the metastasis of human bladder cancer cells by promoting migration and conferring resistance to ferroptosis through activation of PPAR gamma signaling | Elsevier Enhanced Reader. (s. d.). https://doi.org/10.1016/j.freeradbiomed.2022.06.247
34. Luo, L., Xia, L., Zha, B., Zuo, C., Deng, D., Chen, M., Hu, L., He, Y., Dai, F., Wu, J., Wang, C., Wang, Y., & Zhang, Q. (2018). miR-335-5p targeting ICAM-1 inhibits invasion and metastasis of thyroid cancer cells. *Biomed Pharmacother, 106*, 983-990. https://doi.org/10.1016/j.biopha.2018.07.046
35. Marinelli, O., Morelli, M. B., Annibali, D., Aguzzi, C., Zeppa, L., Tuyaerts, S., Amantini, C., Amant, F., Ferretti, B., Maggi, F., Santoni, G., & Nabissi, M. (2020). The Effects of Cannabidiol and Prognostic Role of TRPV2 in Human Endometrial Cancer. *International Journal of Molecular Sciences, 21*(15), Article 15. https://doi.org/10.3390/ijms21155409
36. Massi, P., Solinas, M., Cinquina, V., & Parolaro, D. (2013). Cannabidiol as potential anticancer drug. *British Journal of Clinical Pharmacology, 75*(2), 303-312.
37. MiR-335-5p targeting ICAM-1 inhibits invasion and metastasis of thyroid cancer cells | Lecteur amélioré Elsevier. (s. d.). https://doi.org/10.1016/j.biopha.2018.07.046
38. Molecularly targeted anti-cancer drugs inhibit the invasion and metastasis of hepatocellular carcinoma by regulating the expression of MMP and TIMP gene families | Lecteur amélioré Elsevier. (s. d.). https://doi.org/10.1016/j.bbrc.2018.08.203
39. Muthusami, S., Sabanayagam, R., Periyasamy, L., Muruganantham, B., & Park, W. Y. (2022). A review on the role of epidermal growth factor signaling in the development, progression and treatment of cervical cancer. *Int J Biol Macromol, 194*, 179-187. https://doi.org/10.1016/j.ijbiomac.2021.11.117
40. Seltzer, E. S., Watters, A. K., MacKenzie, D., Granat, L. M., & Zhang, D. (2020). Cannabidiol (CBD) as a Promising Anti-Cancer Drug. *Cancers, 12*(11), E3203. https://doi.org/10.3390/cancers12113203
41. Sharafi, G., He, H., & Nikfarjam, M. (2019). Potential Use of Cannabinoids for the Treatment of Pancreatic Cancer. *Journal of Pancreatic Cancer, 5*(1), 1‑7. https://doi.org/10.1089/pancan.2018.0019
42. Singh, M., Thakur, M., Mishra, M., Yadav, M., Vibhuti, R., Menon, A. M., Nagda, G., Dwivedi, V. P., Dakal, T. C., & Yadav, V. (2021). Gene regulation of intracellular adhesion molecule-1 (ICAM-1): A molecule with multiple functions. *Immunol Lett, 240*, 123-136. https://doi.org/10.1016/j.imlet.2021.10.007
43. Tabti, K., Hajji, H., Sbai, A., Maghat, H., Bouachrine, M., & Lakhlifi, T. (2023). Identification of a Potential Thiazole Inhibitor Against Biofilms by 3D QSAR, Molecular Docking, DFT Analysis, MM-PBSA Binding Energy Calculations, and Molecular Dynamics Simulation. *Physical Chemistry Research*, 369‑389. https://doi.org/10.22036/pcr.2022.335657.2068
44. The oncogenic lysophosphatidylinositol (LPI)/GPR55 signaling | Lecteur amélioré Elsevier. (s. d.). https://doi.org/10.1016/j.lfs.2022.120596
45. Ye, D., Xu, H., Tang, Q., Xia, H., Zhang, C., & Bi, F. (2021). The role of 5-HT metabolism in cancer. *Biochimica et Biophysica Acta - Reviews on Cancer, 1876*(2), 188618.